COMMUNICATIONS IN SCIENCE AND TECHNOLOGY
Homepage: cst.kipmi.or.id

Utilizing *Pometia Pinnata* leaf extract in microwave synthesis of ZnO nanoparticles: Investigation into photocatalytic properties

Ari Sulistyo Rini[a,*] Yolanda Rati[b], Gema Maheta[a], Arie Purnomo Aji[a], Saktioto[a]

[a]*Department of Physics, University of Riau, Pekanbaru 28293, Indonesia*
[b]*Department of Physics, Bandung Institute of Technology, Bandung 40132, Indonesia*

Article history:
Received: 9 March 2024 / Received in revised form: 6 June 2024 / Accepted: 9 June 2024

Abstract

In this work, ZnO photocatalyst has been synthesized using matoa (*Pometia pinnata*) leaf extract under various microwave irradiation powers at 360, 540, and 720 Watts for 3 minutes on each. The UV-Vis absorption spectra of ZnO exhibited a peak in the ultraviolet region 300-360 nm. UV-Vis absorption analysis revealed a decrease in the band gap energy from 3.15 eV to 3.10 eV as the irradiation power increased. Field emission scanning electron microscopy (FESEM) images displayed spherical and nanoplatelet morphology with a decrease in particle size observed from 773 to 709 nm with increasing irradiation power. X-ray diffraction (XRD) analysis confirmed the hexagonal wurtzite structure of ZnO with crystallite sizes in the range of ~18-20 nm. The synthesized ZnO nanoparticles was successfully employed as a photocatalyst in 4-nitrophenol degradation, achieving the highest degradation percentage of 82.7% at 540 Watts with a corresponding reaction rate constant of 0.0126/min. In conclusion, the microwave-assisted synthesis of ZnO using on matoa leaf extract demonstrated significant potential for the degradation of organic pollutants, thereby contributing to water purification efforts.

Keywords: 4-nitrophenol; matoa leaf extract; irradiation power; zinc oxide

1. Introduction

Global concern about water pollution is increasing every year. The textile, paper, and pharmaceutical sectors are primarily responsible for the issues that lead to water contamination. 129 carcinogenic organic chemicals from industrial waste have, at least, been found [1]. Due to its widespread use and excellent stability, 4-nitrophenol ($C_6H_5NO_3$) is one of the primary components in organic waste and is, therefore, challenging to break down [2]. Consequently, the pollutant 4-nitrophenol is a global priority to be decomposed and regulated with recommended levels in water at levels ranging from 1 to 20 ppb [3].

Various methods have been used to address pollution in aquatic ecosystem, including microbial catabolism, Fenton, biodegradation, and electrochemical processes [4]. Nevertheless, these methods are considered ineffective for still leaving byproducts that are harmful to the environment. In addition, the operational and maintenance costs for the equipment are high [5]. An advanced oxidation process (AOP) based on semiconductor photocatalysts is a viable choice for pollutants degradation. In the AOP process, photons are employed to accelerate the reaction. This process is considered environmentally benign and able to mineralize contaminants without generating any by-products [6].

Semiconductor materials can absorb UV and visible radiation very well [7]. Metal oxides and metal sulfides semiconductor are extensively utilized in photocatalytic reactions. ZnO particularly can absorb a broad light spectrum, possesses high electron mobility, and has a high redox potential [8]. Its narrow band gap (~ 3.37 eV) enables the efficient absorption of the UV spectrum, contributing to its photocatalyst performance. This feature promotes ZnO as superior to TiO_2, which has a wide band gap of 3.70 eV [9].

ZnO can be prepared by a range of procedures such as sol-gel, hydrothermal, precipitation, atomic deposition, and sonochemical methods. Nevertheless, these techniques sometimes need to use the hazardous substances and costly apparatus [10]. Microwave-assisted green synthesis is an effective path as the process is fast, energy-efficient, and environmentally friendly [11]. Microwave irradiation works by transferring energy to the material, which is converted into heat energy [12]. Besides being time efficient, this technique also produces an high purity and controlled particle formation compared to conventional heating technique [13]. Preparation conditions such as pH, temperature, precursor concentration, and the choice of stabilizing agent play a crucial role in controlling material features. Utilizing natural ingredients from plant extracts as a stabilizing agent is advantageous as they

* Corresponding author.
Email: ari.sulistyo@lecturer.unri.ac.id
https://doi.org/10.21924/cst.9.1.2024.1407

contain secondary metabolites such as flavonoids, phenols, and alkaloids, which can replace chemical commercial capping agents such as polyvinylpyrrolidone [14,15]. Lagashetty et al. reported the synthesis of ZnO using banyan *(Ficus benghalensis*) leaf extract with 800-watt irradiation producing spherical particle with an average diameter of 42 nm [16]. Furthermore, the ZnO synthesized with watermelon peel extract demonstrated high performance photocatalytic activity [17].

In this study, we investigated the effect of microwave irradiation power on the optic, morphology, and structure of ZnO synthesized using matoa (*Pometia pinnata*) leaf extract. Previous studies have utilized plants extract for the green synthesis of ZnO, often involving traditional heating methods or commercial reagents that are less environmentally friendly [10,14]. The integration of microwave synthesis in this study represents a significant advancement, offering a rapid, energy-efficient and uniform heating process that enhances the quality and functionality of ZnO nanoparticles.

Matoa leaf extract, in particular, contains the high levels of flavonoids (phenols) and antioxidants, providing superior stabilization and capping properties compared to other natural resources [19]. ZnO based on matoa leaf extract has been previously reported using the laser ablation method for antibacterial applications [18] and demonstrated excellent photodegradation against methylene blue dye [19]. However, the removal of 4-nitrophenol pollutants by ZnO based on matoa leaf extract has not been previously reported. This dual approach not only emphasizes the green synthesis but also improves the photocatalytic performance of ZnO, making it a more viable option for environmental remediation applications.

2. Materials and Methods

2.1. Green synthesis of ZnO

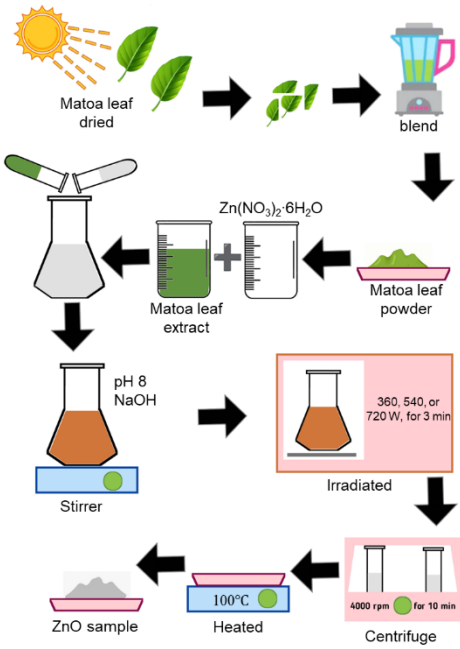

Fig. 1. The schematic process of ZnO synthesis based matoa leaf extract

Fig. 1 depicts the mechanism of ZnO biosynthesis. It began by drying the fresh matoa leaves in the sunlight, mashed with a blender, and filtered using a sieve. About 1 g of matoa leaf powder was heated at 100°C in a beaker glass filled with 50 ml of water for 10 minutes. The extract was then filtered using Whatman paper no. 1. For the preparation of ZnO, zinc nitrate hexahydrate precursor was prepared at a concentration of 50mM. In a 250mL Erlenmeyer, 40 ml of this solution was reacted with 10ml of extract at pH 8. Furthermore, it was irradiated in a microwave oven for 3 minutes at different powers, including 360, 540, and 720 Watts, centrifuged at 4000 rpm and dried at 100°C. Each ZnO sample was named as Znpp-xxx according to its irradiation power (xxx) where Znpp came from ZnO and *pometia pinnata*.

2.2. Characterization

The optical absorption was analyzed by means of a UV-Vis SHIMADZU spectrophotometer in the wavelength range of 300-600 nm. The crystalline structure was characterized by a Rigaku MiniFlex 600 diffractometer at the range of 2θ = 20-80°. The hexagonal lattice constant (a,c) was calculated by:

$$1/{d_{hkl}}^2 = 4(h^2 + hk + k^2)/3a^2 + 1^2/3c^2 \quad (1)$$

where d_{hkl} is the distance between (hkl) plane from Bragg's equation:

$$d_{hkl} = \lambda/2\sin\theta \quad (2)$$

and the crystallite size (D) was calculated using the Debye Scherrer formula:

$$D = k\lambda/\beta\cos\theta \quad (3)$$

where k is Scherrer constant (0.9), λ represents the wavelength of Cukα = 1.541 Å, and β denotes the full width at half maximum (FWHM). Field Emission Scanning Electron Microscope (FESEM) model Quanta FEG 650 was used to investigate surface morphology at a magnification of 25,000 times.

2.3. Photocatalytic test

The application of ZnO as a photocatalyst was examined in the degradation reaction of the pollutant 4-nitrophenol. About 5 mg of ZnO was diluted into 50 ml of 4-nitrophenol solution (5 ppm), and it was observed under a UV-C lamp for 2 hours. In every 20 minutes, 3 mL of the test solution was taken to measure the absorption spectrum using a Cary 60-type UV-Vis spectrophotometer.

3. Results and Discussion

3.1. UV-Vis Absorption

Fig. 2 presents the absorption spectrum in the ZnO-based matoa leaf extract's ultraviolet-visible region with various irradiation powers. The absorption peaks of each sample, Znpp-360, Znpp-540, and Znpp-720, were obtained at a wavelength of 360 nm, 359 nm, and 358 nm. The formation of ZnO nanoparticles is shown by the peaks in this area [20].

The highest absorption peak shifted toward a shorter wavelength as the irradiation power rose (blueshift). It was correlated to the decrease in particle size and increase in photon

energy [21]. Low absorption was obtained in the visible region (380–600 nm) for all samples. Yusof et al. observed similar outcomes as well [22]. Optical absorption at a wavelength of 360 nm proved a maximum photon energy of 3.37 eV (band gap), which is required for electrons to be excited from the valence band to the conduction band.

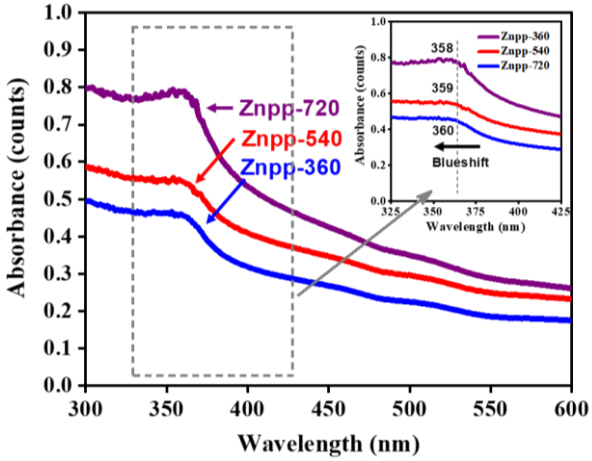

Fig. 2. The absorption spectrum of ZnO at different power irradiation

Fig. 3 presents the determination curve of ZnO band gap energy with various irradiation powers. Each sample had the band gap energy of 3.15 eV, 3.13 eV, and 3.10 eV for the Znpp-360, Znpp-540, and Znpp-720, respectively. A narrower band gap energy was resulted from an increase in irradiation. It indicated that irradiation determined the electronic structure of the material. The irradiation released more carriers, which made the Fermi level closer to the conduction band and reduced the energy gap [23]. Green synthesis's obtained band gap energy was lower than the physical-chemical process ZnO, i.e., 3.39 eV [24].

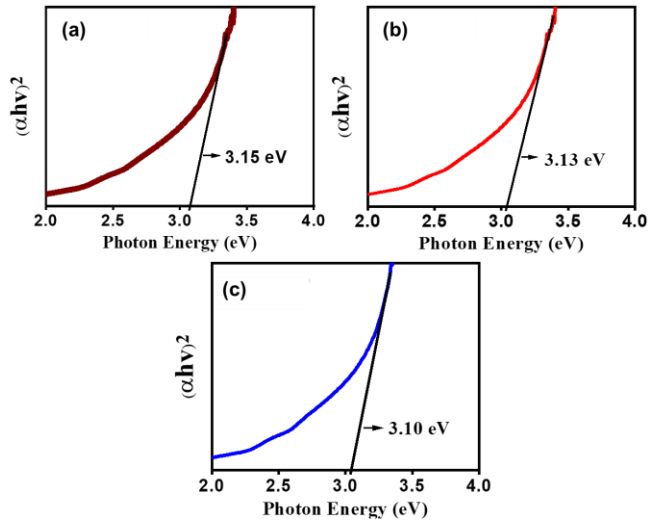

Fig. 3. Band gap energy curve of ZnO at different power irradiation (a) Znpp-360, (b) Znpp-480, and (c) Znpp-720

3.2. FESEM Morphology

Fig. 4 exhibits FESEM images identifying the surface morphology of the ZnO-based matoa leaf extract with various irradiation powers. The predominant particle shape of the ZnO was spherical. The spherical and clustered surface form proved the successful formation of ZnO particles [10]. In addition, some nanoplatelets accumulated. A similar morphology has been reported by Alharthi et al. on ZnO green synthesis using *Ziziphus jujuba* leaf extract by the microwave method [13].

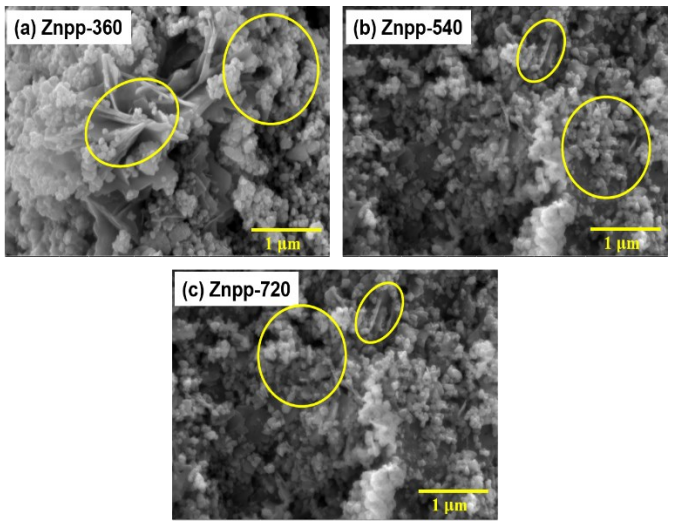

Fig. 4. FESEM images of ZnO at different power irradiation

The Znpp-360, Znpp-540, and Znpp-720 had the particle sizes of 773.0, 743.9, and 709.2 nm, respectively. ZnO particle size decreased as the microwave irradiation power rose. The intensity of irradiation power increased the formation of crystals and facilitated particle collisions making the particle size decreased [25]. It aligned with the band gap energy as previously discussed. The band gap energy narrowed with increasing irradiation, reducing particle size.

3.3. XRD Structure

Fig. 5 shows the X-ray diffraction (XRD) pattern of the ZnO with various irradiation powers. The diffractogram spectrum indicated seven characteristic peaks that confirmed the crystalline phase of ZnO. Each diffraction peak at 2θ= 31.7°, 34.4°, 36.2°, 47.5°, 56.6°, 62.8°, and 67.9° represented the hkl plane (100), (002), (101), (102), (110), (103), (112), respectively. The XRD pattern revealed a hexagonal wurtzite structure that matched data from the Joint Committee on Powder Diffraction Studies Standards (JCPDS no. 34-1451) [15]. High diffraction intensity was obtained from ZnO green synthesis, prepared using meta leaf extract as a stabilizer. The strong diffraction peaks attested to the high crystallinity. Additionally, this phase demonstrated the high ZnO purity because there were no diffraction peaks from residues or impurities. Microwave heating with higher radiation power produced better crystallinity properties, as seen from the increasing diffraction intensity. Microwaves speed up reactions to produce better structures [26].

Table 1 presents the XRD parameters data, including interplanar spacing, lattice constant, and crystallite size. The lattice constants obtained aligned with the ZnO produced by physical methods with a = 5.21 Å and c = 3.25 Å [27]. The crystallite size was calculated using the Debye-Scherrer equation, $D=0.9\lambda/2\beta\cos\theta$. The crystallite size only slightly increased with rising irradiation power. The average crystallites formed had a size of about 20 nm. It was close to the one previously reported, which studied Cassia auriculate leaf extract-mediated ZnO [28].

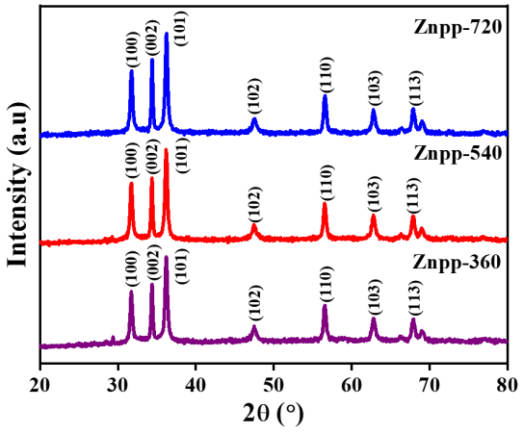

Fig. 5. Diffractogram pattern of ZnO at different power irradiation

Table 1. Lattice parameter and crystallite size of ZnO at different power irradiation

Sample	d-spacing (Å)	Lattice constant (Å)		Crystallite size (nm)
		a (Å)	c (Å)	
Znpp-360	2.480	5.217	3.254	18.795
Znpp-540	2.480	5.221	3.261	19.340
Znpp-720	2.478	5.213	3.253	19.958

3.4. Photocatalytic Activity

The photocatalyst process using ZnO-based matoa leaf extract against 5 ppm 4-nitrophenol pollutant has been successfully evaluated. As shown in Fig. 6(a), 4-nitrophenol color changed from light yellow to colorless. The absorbance peak at 400 nm represented the absorption characteristic of 4-nitrophenol [29]. The curve of A/A_0 versus irradiation time in Fig. 6(b) illustrated the decrease in 4-nitrophenol concentration every 20 minutes during the photocatalyst test. Each sample showed a significant decrease in 4-NP concentration though the differences between them were not entirely distinct. The decrease in the curve proved that the ZnO green synthesis has been successful in the 4-nitrophenol degradation process. The photocatalyst mechanism involved the pairs of electrons and holes reacting on oxygen (O_2) and water (H_2O) to produce superoxide ($\cdot O_2$) and hydroxyl radicals ($\cdot OH$). The hydroxyl radicals reacted to reduce the reactants in pollutants, generating 4-aminophenol as a decomposed substance that is less hazardous in water [5].

To evaluate the kinetics of photocatalytic reaction, the relation of $\ln(A/A_0)$ versus time was plotted, as depicted in Fig. 6(c). The reaction kinetics of the ZnO photocatalyst adhered to the pseude-first-order kinetic equation, $\ln(A/A_0) = -kt$ where the slope of the curve represented the reaction rate constant (k) [17]. The reaction rate constants of the Znpp-360, Znpp-540, and Znpp-720 samples were 0.0129/min, 0.0126/min, and 0.0114/min, respectively. These constant could be used to calculate the minimum number of pollutant molecules that would interact with the ZnO catalyst surface during the photocatalytic reaction, affecting the performance of reactive hydroxyl radicals and superoxide [30]. A previous report by Kadam et al. reported a ZnO green synthesis reaction rate constant of 0.00262/min for the p-nitrophenol degradation process [31]. The results of this study are considered comparable as the reaction rate obtained was relatively higher than that of the previous study.

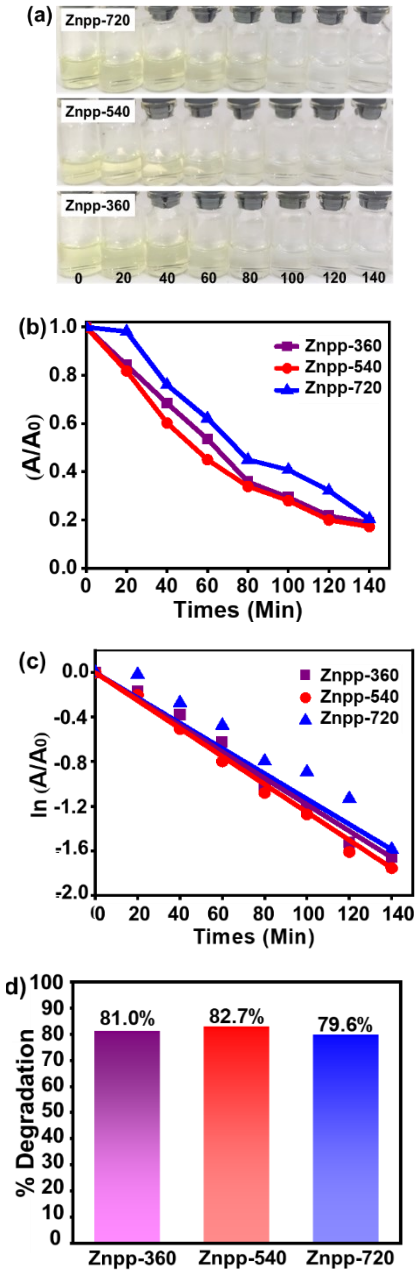

Fig. 6. (a) Photodegradation process of 4-nitrophenol by ZnO sample, (b) Curve of A/A_0 vs. t, (c) $\ln(A/A_0)$ vs. t, and (d) Bar diagram % degradation of ZnO at different power irradiation for 140 min

The degradation percentage describes the performance of the ZnO photocatalyst. Fig. 6(d) presents a bar chart illustrating the % degradation of 4-NP after 140 minutes photocatalyst test. The Znpp-360, Znpp-540, and Znpp-720 achieved the degradation percentage of 81.0%, 82.7%, and 79.6%, respectively. The variation in irradiation power did not significantly affect the efficiency of the photocatalyst. Previous studies have reported the photodegradation of 4-nitrophenol by ZnO prepared using Sentul peel extract, achieving an efficiency of 73.2% [32]. The photocatalyst activity of ZnO in microwave-assisted green synthesis is closely related to its optical and electronic properties. High absorption indicates that ZnO effectively absorbs light, thereby enhancing photocatalyst activity. The narrow energy band gap of the ZnO sample (3.10-3.15 eV) can produce many excited electrons from the valence band [33]. Additionally, a study on ZnO mediated by matoa leaf extract under various irradiation powers demonstrated

exceptional photocatalytic performance.

4. Conclusion

We have studied the physical properties of ZnO prepared using the microwave method mediated by matoa leaf extract. The high irradiation power decreased the energy gap and particle size. Meanwhile, surface morphology showed spherical and nanoplatelet shapes. The average crystallite size of ZnO was 19-20 nm. Increasing the irradiation power did not significantly affect the degradation performance of 4-nitrophenol. A change in the color of the pollutant from yellow to colorless has been investigated. In addition, the degradation percentage obtained exceeded 80%, which is suitable for developing wastewater treatment applications.

Acknowledgements

The authors express their gratitude to the Directorate General of Research, Technology, and Community Service, Ministry of Culture and Education, Republic of Indonesia, and the Institute for Research and Community Service, University of Riau, for their generous financial support and invaluable facilitation throughout this research endeavor.

References

1. B. Surya, H. Hamsina, R. Ridwan, B. Baharuddin, F. Menne, A. T. Fitriyah, et al., *The complexity of space utilization and environmental pollution control in the main corridor of Makassar City, South Sulawesi, Indonesia,* Sustain. 12 (2020) 1-41.
2. A. A. Yahya, K. T. Rashid, M. Y. Ghadbhan, N. E. Mousa, H. S. Majdi, I. K. Salih, et al., *Removal of 4-nitrophenol from aqueous solution by using polyphenylsulfone-based blend membranes: Characterization and performance,* Membrans 11 (2021) 1-20.
3. Y. Qin, H. Zhang, Z. Tong, Z. Song, and N. Chen, *A facile synthesis of Fe_3O_4@SiO_2@ZnO with superior photocatalytic performance of 4-nitrophenol*, J. Environ. Chem. Eng. 5 (2017) 2207-2213.
4. K. Qi, B. Cheng, J. Yu, and W. Ho, *Review on the improvement of the photocatalytic and antibacterial activities of ZnO*, J. Alloys Compd, 727 (2017) 792–820.
5. P. Deka, R. C. Deka, and P. Bharali, *In situ generated copper nanoparticle catalyzed reduction of 4-nitrophenol*, New J. Chem. 38 (2014) 1789–1793.
6. A. Hameed, M. Aslam, I. M. I. Ismail, S. Chandrasekaran, M. W. Kadi, and M. A. Gondal, *Sunlight assisted photocatalytic mineralization of nitrophenol isomers over W^{6+} impregnated ZnO*, Appl. Catal. B Environ. 160–161 (2014) 227–239.
7. D. Chen, Y. Cheng, N. Zhou, P. Chen, Y. Wang, K. Li, et al., *Photocatalytic degradation of organic pollutants using TiO_2-based photocatalysts: A review,* J. Clean. Prod. 268 (2020) 121725.
8. L. C. Chen and Z.L. Tseng, *ZnO-Based Electron Transporting Layer for Perovskite Solar Cells,* Nanostructured Sol. Cells, 1 (2017) 203–215.
9. Z. Wang, X. Zhu, J. Feng, C. Wang, C. Zhang, X. Ren, et al., *Antisolvent-and Annealing-Free Deposition for Highly Stable Efficient Perovskite Solar Cells via Modified ZnO*, Adv. Sci. 8 (2021) 1–7.
10. D. Sharma, M. I. Sabela, S. Kanchi, P. S. Mdluli, G. Singh, T. A. Stenstrom, et al., *Biosynthesis of ZnO nanoparticles using Jacaranda mimosifolia flowers extract: Synergistic antibacterial activity and molecular simulated facet specific adsorption studies,* J. Photochem. Photobiol. B Biol. 162 (2016) 199–207.
11. M. Shakibaie, S. Riahi-Madvar, A. Ameri, P. Amiri-Moghadam, M. Adeli-Sardou, and H. Forootanfar, *Microwave Assisted Biosynthesis of Cadmium Nanoparticles: Characterization, Antioxidant and Cytotoxicity Studies,* J. Clust. Sci. 33 (2021) 1877-1887.
12. L. Ni'Mah, S. R. Juliastuti, and M. Mahfud, *One-stage microwave-assisted activated carbon preparation from Langsat peel raw material for adsorption of iron, manganese and copper from acid mining waste*, Commun. Sci. Technol. 8 (2023) 143–153.
13. M. N Alharthi, I. Ismail, S. Bellucci, N. H Khdary, and M. Abdel Salam, *Biosynthesis microwave-assisted of zinc oxide nanoparticles with ziziphus jujuba leaves extract: Characterization and photocatalytic application,* Nanomaterials, 11 (2021) 1682.
14. D. A. Ramdhani, W. Trisunaryanti, and Triyono, *Study of green and sustainable heterogeneous catalyst produced from Javanese Moringa oleifera leaf ash for the transesterification of Calophyllum inophyllum seed oil,* Commun. Sci. Technol. 8 (2023) 124–133.
15. .N. Kumar, K. Sakthivel, and V. Balasubramanian, *Microwave assisted biosynthesis of rice shaped ZnO nanoparticles using Amorphophallus konjac tuber extract and its application in dye sensitized solar cells,* Mater. Sci. Pol. 35 (2017) 111–119.
16. A. Lagashetty, S. K. Ganiger, P. R. K., S. Reddy, and M. Pari, *Microwave-assisted green synthesis, characterization and adsorption studies on metal oxide nanoparticles synthesized using: Ficus Benghalensis plant leaf extracts*, New J. Chem., 44 (2020) 14095–14102.
17. A. S. Rini, Y. Rati, R. Fadillah, R. Farma, L. Umar, and Y. Soerbakti, *Improved Photocatalytic Activity of ZnO Film Prepared via Green Synthesis Method Using Red Watermelon Rind Extract*, Evergreeen. 9 (2022) 1046–1055.
18. N. Yudasari, P. A. Wiguna, W. Handayani, M. M. Suliyanti, and C. Imawan, *The formation and antibacterial activity of Zn/ZnO nanoparticle produced in Pometia pinnata leaf extract solution using a laser ablation technique,* Appl. Phys. A Mater. Sci. Process. 127 (2021) 1–11.
19. A. S. Rini, Y. Rati, R. Dewi, and S. Putri, *Investigating the Influence of Precursor Concentration on the Photodegradation of Methylene Blue using Biosynthesized ZnO from Pometia pinnata Leaf Extracts,* Baghdad Sci. J. 20 (2023) 2532–2539.
20. A. A. Elrefaey, A. D. El-Gamal, S. M. Hamed, and E. F. El-Belely, *Algae-mediated biosynthesis of zinc oxide nanoparticles from Cystoseira crinite (Fucales; Sargassaceae) and it's antimicrobial and antioxidant activities,* Egypt. J. Chem. 65 (2022) 231–240.
21. J. Wojnarowicz, T. Chudoba, S. Gierlotka, and W. Lojkowski, *Effect of microwave radiation power on the size of aggregates of ZnO NPs prepared using microwave solvothermal synthesis,* Nanomaterials, 8 (2022) 343.
22. H. Mohd Yusof, N. A. Abdul Rahman, R. Mohamad, U. H. Zaidan, and A. A. Samsudin, *Biosynthesis of zinc oxide nanoparticles by cell-biomass and supernatant of Lactobacillus plantarum TA4 and its antibacterial and biocompatibility properties*, Sci. Rep. 10 (2020) 1–13.
23. G. M. Abdelghani, A. Ben Ahmed, and A. B. Al-Zubaidi, *Synthesis, characterization, and the influence of energy of irradiation on optical properties of ZnO nanostructures,* Sci. Rep. 12 (2022) 1–17.
24. M. Zare, K. Namratha, K. Byrappa, D. M. Surendra, S. Yallappa, and B. Hungund, *Surfactant assisted solvothermal synthesis of ZnO nanoparticles and study of their antimicrobial and antioxidant properties*, J. Mater. Sci. Technol. 34 (2018) 1035–1043.
25. N. Pauzi, N. M. Zain, and N. A. A. Yusof, *Microwave-assisted Synthesis of ZnO Nanoparticles Stabilized with Gum Arabic: Effect of microwave irradiation time on ZnO nanoparticles size and morphology*, Bull. Chem. React. Eng. & Catal., 14 (2019) 182–188.
26. G. B. Dudley, A. E. Stiegman, and M. R. Rosana, *Correspondence on microwave effects in organic synthesis*, Angewandte Chemie, 31 (2013)

8074-8079.

27. K. Kandpal, J. Singh, N. Gupta, and C. *Shekhar, Effect of thickness on the properties of ZnO thin films prepared by reactive RF sputtering,* J. Mater. Sci. Mater. Electron. 29 (2018) 14501–14507.
28. P. Ramesh, K. Saravanan, P. Manogar, J. Johnson, E. Vinoth, and M. Mayakannan, *Green synthesis and characterization of biocompatible zinc oxide nanoparticles and evaluation of its antibacterial potential*, Sens. Bio-Sensing Res. 31 (2021) 100399.
29. E. Menumerov, R. A. Hughes, and S. Neretina, *Catalytic Reduction of 4-Nitrophenol: A Quantitative Assessment of the Role of Dissolved Oxygen in Determining the Induction Time*, Nano Lett. 16 (2016) 7791–7797.
30. J. Kou, C. Lu, J. Wang, Y. Chen, Z. Xu, and R. S. Varma, *Selectivity Enhancement in Heterogeneous Photocatalytic Transformations,* Chem. Rev. 117 (2017) 1445–1514.
31. V. V. Kadam, S. D. Shanmugam, and J. P. Ettiyappan, *Photocatalytic degradation of p-nitrophenol using biologically synthesized ZnO nanoparticles*, Environmental Science and Pollution Research. 28 (2021) 12119-12130.
32. A. S. Rini, A. P. Aji, and Y. Rati, *Microwave-assisted biosynthesis of flower-shaped ZnO for photocatalyst in 4-nitrophenol degradation*, Commun. Sci. Technol. 7 (2022) 135–139.
33. X. Bai, L. Li, H. Liu, L. Tan, T. Liu, and X. Meng, *Solvothermal Synthesis of ZnO Nanoparticles for and p-Nitrophenol*, ACS applied materials & interfaces, 7 (2015) 1308-1317.